

# A convenient Mn<sup>III</sup> starting material for the synthesis of homo- and heterometallic manganese carboxylate clusters: Mn<sub>9</sub> and Mn<sub>10-x</sub>Fe<sub>x</sub> complexes

Christos Lampropoulos, Theocharis C. Stamatatos, Khalil A. Abboud, George Christou \*

Department of Chemistry, University of Florida, Gainesville, FL 32611-7200, USA

## ARTICLE INFO

### Article history:

Available online 26 December 2008

### Keywords:

Crystal structures  
Manganese(III) clusters  
Iron(III) clusters  
Molecular wheels  
Carboxylate ligands  
Magnetochemistry

## ABSTRACT

The use of a convenient source of Mn<sup>III</sup> ions, namely the [Mn(OR)(O<sub>2</sub>CR')<sub>2</sub>]<sub>n</sub> (R = H, Me, and R' = Me, Bu<sup>t</sup>) family of 1-D coordination polymers, afforded two new enneanuclear and decanuclear molecular clusters, homometallic [Mn<sub>9</sub>O<sub>7</sub>(O<sub>2</sub>CBu<sup>t</sup>)<sub>13</sub>(MeCN)<sub>2</sub>] (3) and heterometallic [Mn<sub>10-x</sub>Fe<sub>x</sub>(OMe)<sub>20</sub>(O<sub>2</sub>CMe)<sub>10</sub>] (x < 10) (4), respectively. Compound 3 was synthesized by a solvent-induced structural transformation, whereas complex 4 resulted from the reaction of [Mn(OH)(O<sub>2</sub>CMe)<sub>2</sub>]<sub>n</sub> with an Fe<sup>III</sup> source. The core of 3 comprises two [Mn<sub>4</sub>O<sub>2</sub>]<sup>8+</sup> butterfly units and a [Mn<sub>3</sub>O]<sup>7+</sup> triangular unit fused together by sharing one Mn atom. Magnetic susceptibility measurements of 3 revealed dominant antiferromagnetic interactions within the molecule, and a ground state of S = 1 with many low-lying excited states. Complex 4 is a mixed Fe<sup>III</sup>/Mn<sup>III</sup> single-strand molecular wheel, which forms 3D nanotubular stacks arranged in a zig-zag fashion. The described work suggests that the [Mn(OR)(O<sub>2</sub>CR')<sub>2</sub>]<sub>n</sub> compounds represent excellent starting materials for Mn<sup>III</sup> carboxylate cluster chemistry.

© 2008 Elsevier Ltd. All rights reserved.

## 1. Introduction

Nanotechnology has been the focal point of many research projects worldwide over the last decade or so, for reasons including environmental concerns, fuel economy, the need for increased computational power, and high-density information storage, among others [1]. For the latter two cases, nanomagnets have been proposed as viable future solutions. The field of single-molecule magnetism, developed as a molecular approach to nanomagnetism, involves zero-dimensional, polynuclear transition-metal assemblies with a high ground state spin (S) and large axial anisotropy that behave as nanoscale magnets below a blocking temperature (T<sub>B</sub>) [2,3]. Most such species are clusters incorporating Mn<sup>III</sup> ions [3a–c], and this is consistent with the axial Jahn–Teller (JT) elongation of a d<sup>4</sup> ion in octahedral geometry, which is a source of significant single-ion magnetoanisotropy. For a polynuclear Mn<sup>III</sup> cluster, parallel (or nearly so) orientation of JT axes on different Mn<sup>III</sup> ions will lead to significant uniaxial molecular anisotropy, which can lead to SMM behavior if the S value is also large enough [4].

There is thus a continuing interest in the development of original synthetic procedures to new high-spin Mn<sup>III</sup> clusters from simple reagents, whether for SMM applications or not. However, in contrast to Fe<sup>III</sup>, there are only a handful of simple, readily available Mn<sup>III</sup> sources, and synthetic chemists have thus been overcoming this problem using four ways: (i) oxidation of Mn<sup>II</sup> salts under basic

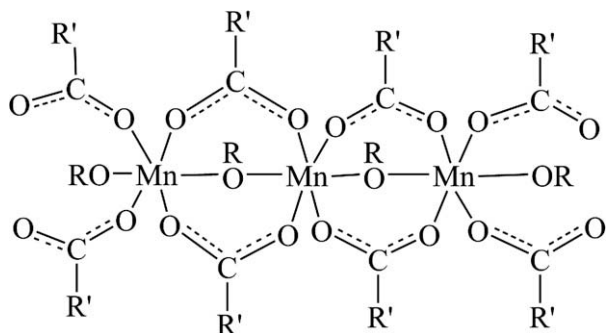
reaction conditions [5], (ii) *in situ* comproportionation reactions between Mn<sup>II</sup> and Mn<sup>VII</sup> reagents [6], (iii) reductive aggregation of Mn<sup>VII</sup> sources under acidic conditions [7], and (iv) use of preformed Mn clusters, which already contain Mn<sup>III</sup> ions [8]. The latter approach requires an extra step of synthesizing the preformed cluster, but this is usually a minor inconvenience and all four strategies are thus convenient and have proved successful in the past. Indeed, the use of preformed species has proved particularly successful employing as starting materials the family of oxo-centered, carboxylate-bridged triangular compounds of general formula [Mn<sub>3</sub>O(O<sub>2</sub>CR)<sub>6</sub>L<sub>3</sub>]<sup>n+</sup> (n = 0, 1; R = various; L = terminal ligands) [8b–d], and more recently the mixed-valence SMM archetype [Mn<sub>12</sub>O<sub>12</sub>(O<sub>2</sub>CR)<sub>16</sub>(H<sub>2</sub>O)<sub>4</sub>] (R = various; 4 Mn<sup>IV</sup>, 8 Mn<sup>III</sup>) [5a,8a]. Herein we report a new and convenient Mn<sup>III</sup> carboxylate starting material for Mn<sup>III</sup> cluster chemistry, which has a 1-D polymer structure (Scheme 1), and which we have used in preliminary work to synthesize a homometallic Mn<sub>9</sub><sup>III</sup> cage and a heterometallic Mn<sub>10-x</sub>Fe<sub>x</sub><sup>III</sup> (x < 10) wheel. Note that derivatives of this family of 1-D polymeric species have been originally reported by Murray and coworkers [9a–c], but never used before as starting reagents for the syntheses of higher nuclearity Mn<sup>III</sup> carboxylate clusters.

## 2. Experimental

### 2.1. General and physical measurements

All manipulations were performed under aerobic conditions using materials (reagent grade) and solvents as received.

\* Corresponding author. Tel.: +1 352 392 6737; fax: +1 352 392 8757.  
E-mail address: [christou@chem.ufl.edu](mailto:christou@chem.ufl.edu) (G. Christou).



**Scheme 1.** A portion of the chain structure of the  $[\text{Mn}^{\text{III}}(\text{OR})(\text{O}_2\text{CR}')_2]_n$  family of polymers.

$\{[\text{Mn}(\text{OH})(\text{O}_2\text{CMe})_2] \cdot 2\text{MeCO}_2\text{H} \cdot \text{H}_2\text{O}\}_n$  (**1**) was prepared as described elsewhere [9d].

Microanalyses (C, H, N) were performed by the in-house facilities of the Chemistry Department at the University of Florida. IR spectra ( $4000\text{--}450\text{ cm}^{-1}$ ) were recorded on a Nicolet Nexus 670 spectrometer with samples prepared as KBr pellets. Variable-temperature dc and ac magnetic susceptibility data were collected at the University of Florida using a Quantum Design MPMS-XL SQUID susceptometer equipped with a 7 T magnet and operating in the 1.8–300 K range. Samples were embedded in solid eicosane to prevent torquing. Pascal's constants were used to estimate the diamagnetic corrections, which were subtracted from the experimental susceptibilities to give the molar paramagnetic susceptibilities ( $\chi_M$ ).

**Table 1**  
Crystallographic data for complexes **3** · toluene, and **4**.

Parameter	<b>3</b> · toluene	<b>4</b>
Formula <sup>a</sup>	$\text{C}_{76}\text{H}_{131}\text{Mn}_9\text{N}_2\text{O}_{33}$	$\text{C}_{40}\text{H}_{90}\text{Fe}_5\text{Mn}_5\text{O}_{40}$
Formula weight ( $\text{g mol}^{-1}$ )	2095.29	1765.07
Crystal system	Monoclinic	Monoclinic
Space group	$C2/c$	$P2_1/c$
$a$ (Å)	45.371(6)	25.747(2)
$b$ (Å)	16.005(2)	15.882(1)
$c$ (Å)	28.249(4)	29.232(2)
$\alpha$ (°)	90	90
$\beta$ (°)	92.165(3)	114.240(2)
$\gamma$ (°)	90	90
$V$ (Å <sup>3</sup> )	20499(5)	10899(2)
$Z$	8	6
$\rho_{\text{calc}}$ ( $\text{g cm}^{-3}$ )	1.358	1.614
Radiation, $\lambda$ (Å) <sup>b</sup>	0.71073	0.71073
Temperature (K)	173(2)	173(2)
$\mu$ ( $\text{mm}^{-1}$ )	1.141	1.892
$R_1$ <sup>c,d</sup>	0.0484	0.0589
$wR_2$ <sup>e</sup>	0.0964	0.1467

<sup>a</sup> Including solvate molecules.

<sup>b</sup> Graphite monochromator.

<sup>c</sup>  $I > 2\sigma(I)$ .

<sup>d</sup>  $R_1 = 100 \sum (|F_o| - |F_c|) / \sum |F_o|$ .

<sup>e</sup>  $wR_2 = 100 \sqrt{\sum [w(F_o^2 - F_c^2)^2] / \sum [w(F_o^2)]^{1/2}}$ ,  $w = 1 / [\sigma^2(F_o^2) + (ap)^2 + bp]$ , where  $p = [\max(F_o^2, 0) + 2F_c^2] / 3$ .

## 2.2. Compound preparation

### 2.2.1. $[\text{Mn}(\text{OMe})(\text{O}_2\text{CBu}^t)_2]_n$ (**2**)

Compound **2** was synthesized following the same procedure as **1**, except that a solvent mixture of MeOH/ $\text{Bu}^t\text{CO}_2\text{H}$  was used in

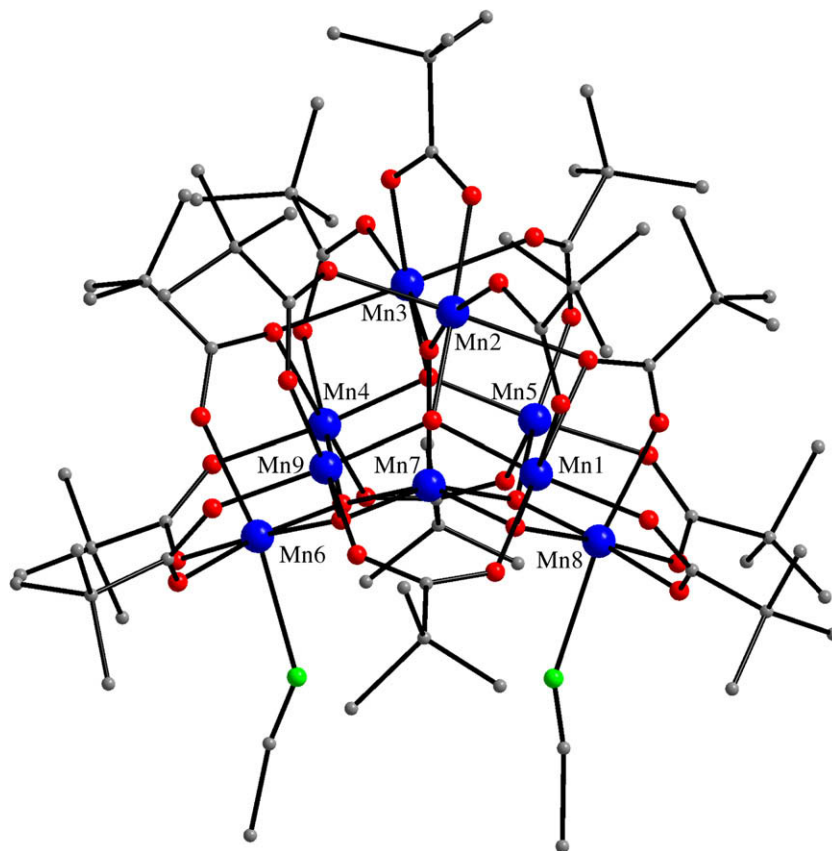


**Fig. 1.** Partially labeled PovRay representation of the structure of **3**, with the hydrogen atoms omitted for clarity. Color code:  $\text{Mn}^{\text{III}}$  blue, O red, N green, C grey. (For interpretation of the references to color in this figure legend, the reader is referred to the web version of this article.)

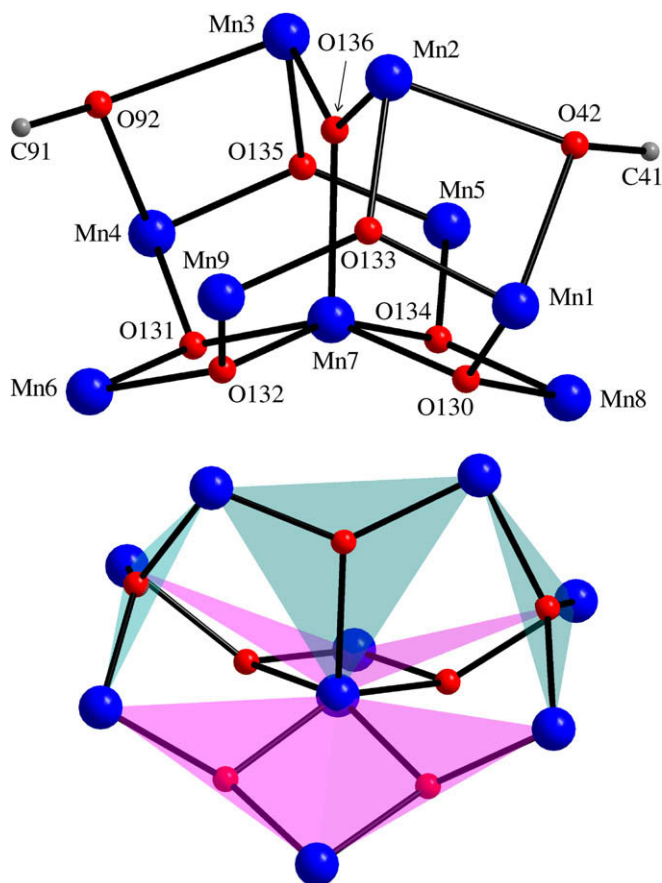


Fig. 2. (Top) PovRay representation of the labeled core of **3**; (bottom) The  $Mn_9$  topology, emphasizing the butterfly  $[Mn_4(\mu_3-O)_2]^{8+}$  and triangular  $[Mn_3(\mu_3-O)]^{7+}$  subcores. Color code:  $Mn^{III}$  blue, O red, C grey.

place of  $H_2O/MeCO_2H$ . The identity of **2** was established by means of IR spectroscopic comparison with authentic material of **1**, and elemental analysis (C, H, N). Yield: 70 % (based on Mn). The dried sample analyzed as solvent-free. *Anal. Calc.* for  $C_{11}H_{21}O_5Mn$ : C, 45.84; H, 7.34; N, 0.00. Found: C, 45.84; H, 7.42; N, 0.01%. Selected IR data (KBr pellet,  $cm^{-1}$ ): 2974s, 1705w, 1576s, 1549s, 1482s, 1406s, 1358s, 1226s, 1003m, 939w, 896w, 785w, 630s, 553s, 459m.

### 2.2.2. $[Mn_9O_7(O_2CBu^t)_{13}(MeCN)_2] \cdot toluene$ (**3** · toluene)

Freshly prepared solid complex **2** (0.20 g, 0.70 mmol) was added to a solution composed of MeCN (25 mL) and toluene (15 mL). The resulting reddish-brown slurry was stirred overnight, during which time most of the solid dissolved, and the color of the solution changed to dark brown. A small quantity of undissolved material was removed by filtration, and the filtrate was allowed to stand undisturbed at room temperature. After 24 h, X-ray quality dark brown crystals of **3** · toluene were collected by filtration, washed with  $Et_2O$  ( $2 \times 5$  ml), and dried under vacuum. Yield: 60% (based on Mn). Material that had been dried under vacuum for 10–12 h and then stored in air was found to have lost the bound MeCN groups, which were replaced with  $H_2O$  molecules; thus, vacuum-dried solid analyzed as  $[Mn_9O_7(O_2CBu^t)_{13}(H_2O)_2]$ . *Anal. Calc.* for  $C_{52}H_{121}O_{35}Mn_9$ : C, 39.89; H, 6.23; N, 0.00. Found: C, 40.28; H, 6.08; N, 0.02%. IR (KBr pellet,  $cm^{-1}$ ): 3853w, 3748w, 3433mb, 2969s, 2921s, 2355m, 1637m, 1558s, 1487s, 1421s, 1370s, 1229s, 1164m, 1114m, 1067mb, 903w, 788w, 692m, 625m.

Table 2

Selected interatomic distances (Å) and bond angles ( $^\circ$ ) for complex **3** · toluene.

Mn1–O133	1.874(3)
Mn1–O130	1.881(3)
Mn1–O12	1.948(3)
Mn1–O31	1.962(3)
Mn1–O2	2.124(3)
Mn1–O42	2.259(3)
Mn2–O136	1.854(3)
Mn2–O133	1.881(3)
Mn2–O62	1.934(3)
Mn2–O32	1.993(3)
Mn2–O52	2.234(3)
Mn2–O42	2.309(3)
Mn3–O136	1.851(3)
Mn3–O135	1.885(3)
Mn3–O61	1.936(3)
Mn3–O81	1.993(3)
Mn3–O71	2.225(3)
Mn3–O92	2.276(3)
Mn4–O135	1.872(3)
Mn4–O131	1.888(3)
Mn4–O112	1.939(3)
Mn4–O82	1.963(3)
Mn4–O102	2.106(4)
Mn4–O92	2.254(3)
Mn5–O135	1.855(3)
Mn5–O134	1.880(3)
Mn5–O22	1.922(3)
Mn5–O72	1.930(3)
Mn5–O101	2.052(4)
Mn6–O131	1.861(3)
Mn6–O132	1.876(3)
Mn6–O122	1.947(3)
Mn6–O111	1.958(3)
Mn6–O91	2.123(4)
Mn6–N2	2.354(5)
Mn7–O134	1.899(3)
Mn7–O132	1.907(3)
Mn7–O130	1.928(3)
Mn7–O131	1.934(3)
Mn7–O136	2.173(3)
Mn8–O130	1.865(3)
Mn8–O134	1.870(3)
Mn8–O21	1.946(3)
Mn8–O11	1.954(3)
Mn8–O41	2.132(3)
Mn8–N1	2.325(4)
Mn9–O133	1.859(3)
Mn9–O132	1.874(3)
Mn9–O51	1.919(3)
Mn9–O121	1.935(3)
Mn9–O1	2.055(3)
O2–Mn1–O42	170.77(12)
O52–Mn2–O42	166.66(12)
O71–Mn3–O92	165.89(12)
O102–Mn4–O92	170.51(13)
O91–Mn6–N2	170.13(15)
O41–Mn8–N1	171.23(16)
Mn8–O130–Mn1	121.99(15)
Mn8–O130–Mn7	97.80(13)
Mn1–O130–Mn7	120.38(15)
Mn6–O131–Mn4	122.57(15)
Mn6–O131–Mn7	97.84(13)
Mn4–O131–Mn7	119.76(14)
Mn9–O132–Mn6	125.54(16)
Mn9–O132–Mn7	120.41(15)
Mn6–O132–Mn7	98.28(13)
Mn9–O133–Mn1	128.45(16)
Mn9–O133–Mn2	123.65(16)
Mn1–O133–Mn2	106.73(13)
Mn8–O134–Mn5	124.94(15)
Mn8–O134–Mn7	98.68(13)
Mn5–O134–Mn7	120.58(15)
Mn5–O135–Mn4	128.81(17)
Mn5–O135–Mn3	123.83(15)
Mn4–O135–Mn3	106.38(14)
Mn3–O136–Mn2	126.60(16)
Mn3–O136–Mn7	116.47(14)

**Table 2** (continued)

Mn2–O136–Mn7	116.91(14)
Mn4–O92–Mn3	83.21(10)
Mn1–O42–Mn2	82.55(10)
Mn1...Mn2	3.0133(11)
Mn3...Mn4	3.0079(11)
Mn6...Mn7	2.8614(9)
Mn7...Mn8	2.8591(10)

**Table 3**Bond valence sum (BVS) calculations for the Mn atoms in **3**.<sup>a</sup>

Atom	Mn <sup>II</sup>	Mn <sup>III</sup>	Mn <sup>IV</sup>
Mn(1)	3.15	<u>3.03</u>	3.18
Mn(2)	3.20	<u>2.93</u>	3.07
Mn(3)	3.22	<u>2.95</u>	3.10
Mn(4)	3.34	<u>3.06</u>	3.21
Mn(5)	3.27	<u>2.99</u>	3.14
Mn(6)	3.35	<u>3.08</u>	3.16
Mn(7)	2.99	<u>2.73</u>	2.87
Mn(8)	3.38	<u>3.10</u>	3.23
Mn(9)	3.27	<u>2.99</u>	3.14

<sup>a</sup> The underlined value is the one closest to the charge for which it was calculated. The oxidation state of a particular atom can be taken as the nearest whole number to the underlined value.

### 2.2.3. $[Mn_{10-x}Fe_x(OMe)_{20}(O_2CMe)_{10}]$ (**4**)

To a slurry of freshly prepared complex **1** (0.50 g, 2.00 mmol) in MeCN (25 mL)/MeOH (1 mL) was added solid  $Fe(NO_3)_3 \cdot 9H_2O$  (0.10 g, 0.25 mmol). The resulting reddish-brown slurry was stirred overnight, during which time most of the solid dissolved and the color of the solution changed to dark brown. A small quantity of undissolved material was removed by filtration, and the filtrate was allowed to stand undisturbed at room temperature. After several days, only a handful of dark brown prismatic crystals of **4** had appeared, and these were devoted solely to single-crystal X-ray diffraction studies.

### 2.3. Single-crystal X-ray crystallography

Data for complexes **3** · toluene and **4** were collected at 173 K on a Siemens SMART PLATFORM equipped with a CCD area detector

and a graphite monochromator utilizing MoK $\alpha$  radiation ( $\lambda = 0.71073 \text{ \AA}$ ). Cell parameters were refined using up to 8192 reflections. A full sphere of data (1850 frames) was collected using the  $\omega$ -scan method (0.3° frame width). The first 50 frames were re-measured at the end of data collection to monitor instrument and crystal stability (maximum correction on  $I$  was <1%). Absorption corrections by integration were applied based on measured indexed crystal faces. The structures were solved by direct methods in SHELXTL6 [10], and refined on  $F^2$  using full-matrix least squares. The non-H atoms were treated anisotropically, whereas the H atoms were placed in ideal positions and refined as riding on their C atoms. Unit cell parameters and structure solution and refinement data are listed in Table 1.

For **3** · toluene, the asymmetric unit contains one Mn<sub>9</sub> cluster and one toluene molecule of crystallization. There are five disordered Bu<sup>t</sup> groups, and each was refined in two parts with their site occupation factors dependently refined. A total of 1071 parameters were refined in the final cycle of refinement using 9621 reflections with  $I > 2\sigma(I)$  to yield  $R_1$  and  $wR_2$  of 4.84 and 9.64%, respectively.

For **4**, the asymmetric unit consists of one and a half M<sub>10</sub> ring located on an inversion center. All metal positions are disordered between Fe and Mn. Each position of the metal on the ring was refined with one Fe and one Mn with their site occupation factors dependently refined in the early refinement stages. All of the site occupation free variables refined to 50%, and thus they were all fixed at 50%. Each position of Fe/Mn metal atoms was constrained to maintain equivalent coordinates and displacement parameters. There are also several disordered methoxy groups where the methyl group was refined in two parts. Several electron density peaks of 2.5 electrons or less were observed around the rings and did not make chemical sense. Most likely, those are a result of ring disorder in the plane of the wheel. A total of 1266 parameters were refined in the final cycle of refinement using 13806 reflections with  $I > 2\sigma(I)$  to yield  $R_1$  and  $wR_2$  of 5.89 and 14.67%, respectively.

## 3. Results and discussion

### 3.1. Syntheses

Slow dissolution with stirring of  $[Mn(OMe)(O_2CBu^t)_2]_n$  (**2**) in MeCN/toluene gave a dark brown solution from which was obtained  $[Mn_9O_7(O_2CBu^t)_{13}(MeCN)_2]$  (**3**) as **3** · toluene in good yields (~60%). The reaction is clearly a hydrolysis involving adventitious water, causing an undoubtedly complicated structural rearrange-

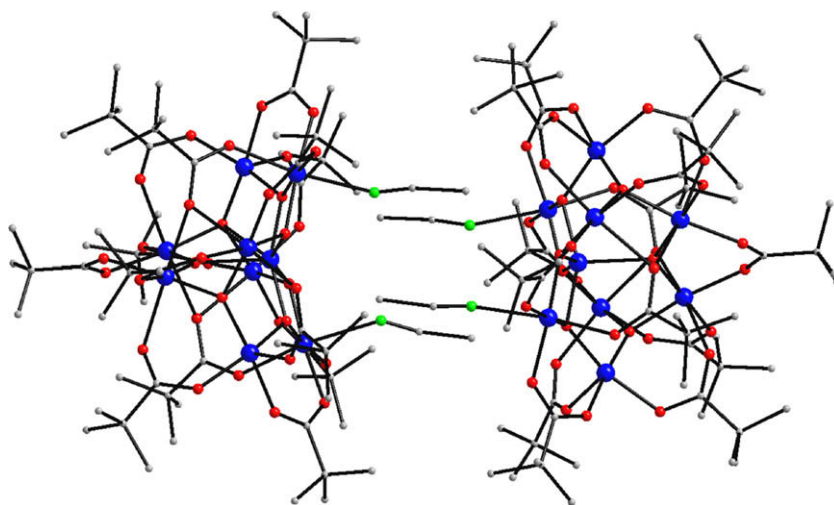


**Fig. 3.** PovRay representation of a pair of Mn<sub>9</sub> cages. Color code: Mn<sup>III</sup> blue, O red, N green, C grey.

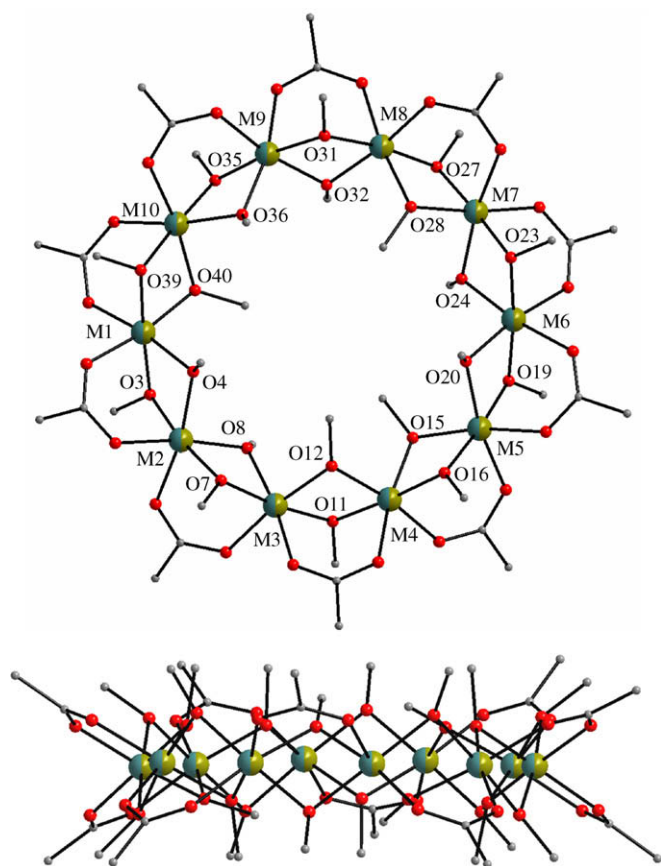


**Fig. 4.** (Top) Labeled PovRay representation of the structure of **4**, with the hydrogen atoms omitted for clarity; (bottom) side-view emphasizing the wheel planarity and O/M/O layered structure. Color code: M (Mn/Fe) blue/green, O red, C grey.

ment but no redox changes since the product contains only  $\text{Mn}^{\text{III}}$  atoms like the starting material **2**. The MeCN is essential for a high-yield transformation; reactions in neat toluene gave only a very low yield ( $\sim 10\%$ ) of a product whose IR spectrum is almost identical with that of **3** and is assumed to be the form with two bound water molecules instead of MeCN. Changes to the exact MeCN:toluene ratio had no effect on the identity of the product, only small changes to the yield. With the identity of **3** established, we also tried similar reactions with  $[\text{Mn}(\text{OH})(\text{O}_2\text{CMe})_2]_n$  (**1**) and, on the basis of IR spectroscopy and elemental analysis data, concluded that the product was the acetate version of **3** and thus did not study this product further. The reaction of **2** in MeCN/MeOH under various conditions yielded the known  $\text{Mn}_{84}$  complex [11], and/or non-crystalline materials difficult to characterize.

We have in the past used complex **1** as the starting material for the preparation of the heterometallic compound  $[\text{CeMn}_8\text{O}_8(\text{O}_2\text{CMe})_{12}(\text{H}_2\text{O})_4]$  [12], and so we now also investigated the use of **1** and **2** in reactions with another 3d metal, namely iron. Thus, the reaction of **1** with  $\text{Fe}(\text{NO}_3)_3 \cdot 9\text{H}_2\text{O}$  in a 8:1 ratio in MeCN/MeOH was explored. It was difficult to isolate pure products from this reaction system, and finally obtained some dark brown crystals in extremely low yields of what proved to be the decanuclear mixed-metal complex  $[\text{Mn}_{10-x}\text{Fe}_x(\text{OMe})_{20}(\text{O}_2\text{CMe})_{10}]$  ( $x < 10$ ) (**4**). The color of the crystalline material **4** clearly precludes assignment of all the metal ions as  $\text{Fe}^{\text{III}}$  ( $x \neq 10$ ) since  $[\text{Fe}_{10}(\text{OMe})_{20}(\text{O}_2\text{CMe})_{10}]$  is a known compound that has a light yellow color. On the other hand, it was also clear that this was not the completely  $\text{Mn}^{\text{III}}$  version  $[\text{Mn}_{10}(\text{OMe})_{20}(\text{O}_2\text{CMe})_{10}]$  ( $x \neq 0$ ). The product thus had to be mixed-metal, but the relative metal content was not possible to be accurately obtained from the refinement of the crystal structure

**Table 4**  
Selected interatomic distances (Å) and bond angles ( $^\circ$ ) for **4**.

M1–O40	1.969(3)
M1–O3	1.974(2)
M1–O39	1.985(2)
M1–O4	2.007(2)
M1–O1	2.033(3)
M1–O38	2.063(2)
M2–O7	1.984(2)
M2–O3	1.986(2)
M2–O4	1.999(2)
M2–O8	2.001(3)
M2–O2	2.040(3)
M2–O5	2.043(2)
M3–O8	1.977(2)
M3–O7	1.984(3)
M3–O12	1.989(2)
M3–O11	1.991(3)
M3–O9	2.032(2)
M3–O6	2.064(2)
M4–O12	1.968(3)
M4–O11	1.979(2)
M4–O16	1.985(2)
M4–O15	2.002(3)
M4–O13	2.038(3)
M4–O10	2.071(3)
M5–O15	1.963(2)
M5–O19	1.988(2)
M5–O16	1.993(3)
M5–O20	2.002(2)
M5–O17	2.024(2)
M5–O14	2.047(3)
M6–O19	1.975(2)
M6–O23	1.978(2)
M6–O20	1.993(3)
M6–O24	2.002(2)
M6–O21	2.040(3)
M6–O18	2.066(2)
M7–O28	1.966(3)
M7–O24	1.991(2)
M7–O23	1.991(2)
M7–O27	1.996(2)
M7–O22	2.040(3)
M7–O25	2.045(3)
M8–O32	1.971(2)
M8–O31	1.976(3)
M8–O28	1.997(2)
M8–O27	2.000(3)
M8–O26	2.023(2)
M8–O29	2.081(2)
M9–O31	1.976(2)
M9–O35	1.980(2)
M9–O36	1.984(3)
M9–O32	2.002(3)
M9–O30	2.038(3)
M9–O33	2.039(3)
M10–O40	1.968(2)
M10–O35	1.976(3)
M10–O39	1.989(3)
M10–O36	1.999(2)
M10–O34	2.039(3)
M10–O37	2.043(2)
M1–O3–M2	99.70(10)
M2–O4–M1	98.15(10)
M3–O7–M2	99.68(11)
M3–O8–M2	99.37(11)
M4–O11–M3	99.24(11)
M4–O12–M3	99.65(11)
M5–O15–M4	99.75(10)
M4–O16–M5	99.30(10)
M6–O19–M5	99.79(11)
M6–O20–M5	98.69(11)
M6–O23–M7	99.43(10)
M7–O24–M6	98.63(10)
M7–O27–M8	98.48(11)
M7–O28–M8	99.58(12)
M8–O31–M9	99.83(11)
M8–O32–M9	99.12(11)
M10–O35–M9	100.07(10)

Table 4 (continued)

M9–O36–M10	99.17(10)
M1–O39–M10	98.36(11)
M10–O40–M1	99.63(11)

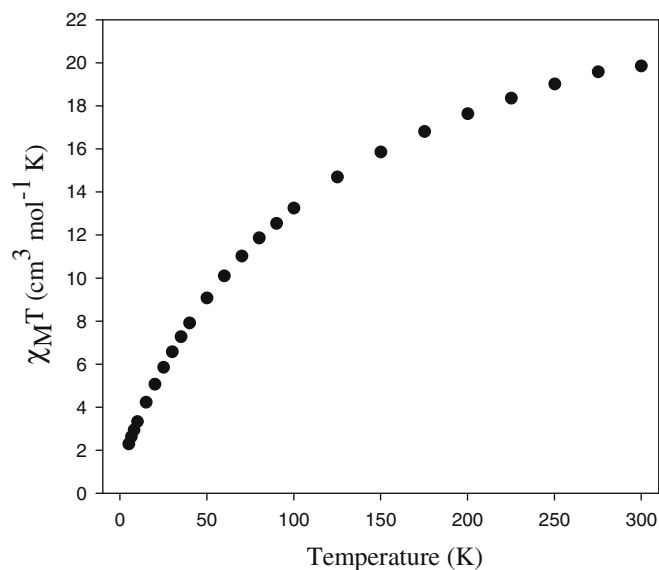
(vide infra). Reasons such as the similar Mn and Fe electronic densities and the complicated overall structure of **4** with a relatively large molecular weight preclude safe conclusions about the exact identity of the metal ions present. Unfortunately, not enough crystals were obtained to allow a metal analysis, and we were unable to increase the yield by varying the solvent ratio. With the identity of **4** established, we also tried to obtain the homometallic  $[\text{Mn}_{10}(\text{O-Me})_{20}(\text{O}_2\text{CMe})_{10}]$  wheel, but were unsuccessful. Reactions of **1** in pure MeOH, for example, gave only uncharacterized  $\text{Mn}^{\text{II}}$  products.

### 3.2. Description of structures

The molecular structure and the core of complex **3** are depicted in Figs. 1 and 2, respectively. Selected interatomic distances and angles are listed in Table 2. Complex **3** contains a  $[\text{Mn}_9\text{O}_7]^{13+}$  core that can be described as two fused  $[\text{Mn}_4\text{O}_2]$  butterflies (Mn1, Mn5, Mn7, Mn8, and Mn4, Mn6, Mn7, Mn9) sharing one Mn atom (Mn7). The remaining two Mn ions (Mn2 and Mn3) are connected to the fused butterfly unit through an  $\text{O}^{2-}$  ion (O136) forming a  $[\text{Mn}_3\text{O}]$  triangle with Mn7. The  $[\text{Mn}_3\text{O}_4]$  base of this unit (Mn6, Mn7 and Mn8) is non-planar, the Mn6–Mn7–Mn8 angle being  $\sim 145^\circ$ . The metal ions are all  $\text{Mn}^{\text{III}}$ , as deduced by consideration of structural parameters and by bond valence sum (BVS) calculations (Table 3) [13]. Atoms Mn5, Mn7, and Mn9 are five-coordinate with distorted square pyramidal geometry ( $\tau = 0.28, 0.09, \text{ and } 0.35$ , where  $\tau$  is 0 and 1 for ideal square pyramidal and trigonal bipyramidal geometries, respectively [14]), and their axial bonds [2.052(4)–2.173(3)] are significantly longer than the basal ones [1.855(3)–1.935(3)]. The remaining Mn atoms are all six-coordinate with distorted octahedral geometries, and display Jahn–Teller axial elongations. Eleven  $\text{Bu}^f\text{CO}_2^-$  groups bind in the common  $\mu$ -bridging mode and two in the rarer  $\mu_3$ -mode, with one O atom bridging two metals. The two MeCN molecules are terminally bound to Mn6 and Mn8.

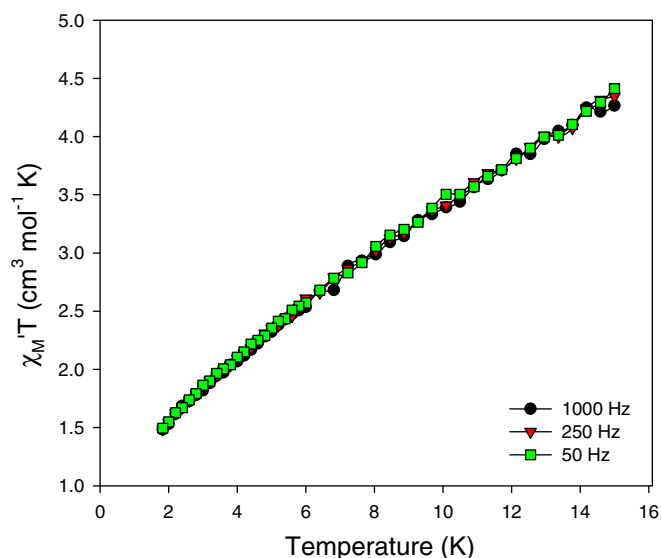
Complex **3** · toluene crystallizes in pairs, as shown in Fig. 3, in a head-to-head arrangement with the MeCN ligands interlocked and the two molecules rotated by  $\sim 90^\circ$  with respect to each other to give an  $S_4$  symmetry dimer. Compounds with a similar core to that in **3** have been previously reported [15], some containing  $\text{Na}^+$  or  $\text{K}^+$  ions, namely  $[\text{Mn}_9\text{Na}_2\text{O}_7(\text{O}_2\text{CPh})_{15}(\text{MeCN})_2]$  [15c] and  $[\text{Mn}_9\text{K}_2\text{O}_7(\text{O}_2\text{CBu}^f)_{15}(\text{HO}_2\text{CBu}^f)_2]$  clusters [15d], respectively; **3** is the third structurally characterized  $\text{Mn}_9$  complex with the general formula  $[\text{Mn}_9\text{O}_7(\text{O}_2\text{CR})_{13}(\text{L})_2]$  ( $\text{R} = \text{Ph}$ ,  $\text{L} =$  terminal ligands, such as pyridine or 2,4-dimethyl-6-hydroxypyrimidine) [15a,8a].

The structure of complex **4** is shown in Fig. 4. Selected interatomic distances and angles are listed in Table 4. The structure is essentially identical to previously characterized  $\text{Fe}_{10}$  ‘ferric wheels’ [16] except that it is clearly a mixed-metal species. Several refinement cycles of the Mn/Fe content led to the conclusion that the compound contains both metals statically disordered about all 10 sites; thus, a general  $\text{Mn}_{10-x}\text{Fe}_x$  ( $x < 10$ ) metal content description was clearly the best fit to the observed electron density. The complex has virtual  $D_{5d}$  symmetry and comprises a near-planar ( $\pm 0.003$ – $0.040$  Å) wheel of 10 octahedral metal atoms with each  $\text{M}_2$  pair bridged by one  $\text{MeCO}_2^-$  and two  $\text{MeO}^-$  groups, giving layers of O atoms above and below the  $\text{M}_{10}$  wheel (Fig. 4, bottom). The wheel has a central hole of  $\sim 3$  Å diameter unoccupied by any guest molecule. The  $\text{M}_{10}$  molecules pack in the crystal on top of each other forming supramolecular nanotubular stacks parallel to the  $a$  axis, but with each molecule slightly tilted relative to this axis.

Fig. 5.  $\chi_M T$  vs.  $T$  plot for complex **3**.

### 3.3. Magnetochemistry

Variable-temperature dc magnetic susceptibility data were collected on a powdered polycrystalline sample of **3**, restrained in eicosane, in a 1 kG (0.1 T) field and in the 5.0–300 K range.  $\chi_M T$  for **3** steadily decreases from  $19.86 \text{ cm}^3 \text{ K mol}^{-1}$  at 300 K to  $2.29 \text{ cm}^3 \text{ K mol}^{-1}$  at 5.00 K (Fig. 5). The rate of decrease increases below  $\sim 50$  K. The room temperature  $\chi_M T$  value is much less than the spin-only value ( $g = 2.0$ ) of  $27 \text{ cm}^3 \text{ K mol}^{-1}$  for nine non-interacting  $\text{Mn}^{\text{III}}$  ions, indicating predominantly strong antiferromagnetic interactions within the molecule and a low, but possibly non-zero, ground state  $S$  value. To determine the ground state of the complex, magnetization data were collected in the magnetic field and temperature ranges 1–60 kG and 1.8–10.0 K. However, we could not get an acceptable fit using data collected over the whole field range, which is a common problem caused by low-lying excited states, especially if some have an  $S$  value greater than that of the ground state. A common solution is to only use data col-

Fig. 6. Plot of the in-phase ( $\chi_M$ ) ac magnetic susceptibility, as  $\chi_M T$  vs.  $T$ , in a 3.5 Oe field oscillating at the indicated frequencies for complex **3**.

lected with low fields ( $\leq 1.0$  T) [5a,5b]. However, it was still not possible to obtain a satisfactory fit assuming that only the ground state is populated in this temperature range. This suggests that the complex possesses particularly low-lying excited states that are populated, even at these relatively low temperatures.

Thus, we turned to ac susceptibility measurements in a 3.5 G ac field oscillating at frequencies in the 50–1000 Hz range. The in-phase  $\chi'_M T$  vs.  $T$  data are shown in Fig. 6 and reveal several pertinent features: (i)  $\chi'_M T$  for **3** decreases linearly with decreasing temperature in the whole temperature range, indicating depopulation of a high-density of low-lying excited states with spin  $S$  greater than that of the ground state, in agreement with the conclusion from the dc studies; (ii) extrapolation of the  $\chi'_M T$  data to 0 K gives a value of  $\sim 1$  cm<sup>3</sup> Kmol<sup>-1</sup> for **3**, indicative of an  $S = 1$  ground state with  $g \sim 2$ . It does appear that the complex does indeed have a non-zero ground state spin, although it could be possible that there are extremely close  $S = 0$ , 1 and even 2 states. In any event, complex **3** clearly has a very small ground state spin. As expected, there were no out-of-phase ac signals down to 1.8 K.

#### 4. Conclusions

The use of the carboxylate-bridged Mn<sup>III</sup> polymeric compound of general formula [Mn(OR)(O<sub>2</sub>CR')<sub>2</sub>]<sub>n</sub> (R = H, Me; R' = Me, Bu<sup>t</sup>) has provided access to two new homo- and heterometallic Mn<sup>III</sup>-based clusters. The homometallic Mn<sub>9</sub> complex **3** has a rare metal core topology, comprising adjacent [Mn<sub>4</sub>O<sub>2</sub>] butterfly and [Mn<sub>3</sub>O] triangular subunits. The heterometallic M<sub>10</sub> (M = Mn/Fe) wheel complex **4** is analogous to the known family of Fe<sub>10</sub> ferric wheels, and clearly contains both Mn and Fe with a varying Mn:Fe ratio. Unfortunately, we have yet to develop a high-yield route to such mixed Mn/Fe wheels to allow us to study this point further, as well as to characterize the magnetic properties, and attempts along this direction are continuing.

#### Acknowledgments

The authors thank the US National Science Foundation (Grant CHE-0414555).

#### Appendix A. Supplementary data

CCDC 704819 and 704818 contain the supplementary crystallographic data for (**3**-toluene) and (**4**). These data can be obtained free of charge via <http://www.ccdc.cam.ac.uk/conts/retrieving.html>, or from the Cambridge Crystallographic Data Centre, 12 Union Road, Cambridge CB2 1EZ, UK; fax: (+44) 1223 336 033; or e-mail: deposit@ccdc.cam.ac.uk. Supplementary data associated with this article can be found, in the online version, at doi:10.1016/j.poly.2008.11.026.

#### References

- [1] Sci. Am. (2001) 285, Special issue on Nanotechnology.
- [2] (a) For reviews, see: G. Christou, D. Gatteschi, D.N. Hendrickson, MRS Bull. 25 (2000) 66; (b) G. Christou, Polyhedron 24 (2005) 2065.

- [3] (a) For some representative references, see: W. Wernsdorfer, N. Aliaga-Alcade, D.N. Hendrickson, G. Christou, Nature 416 (2002) 406; (b) S. Hill, R.S. Edwards, N. Aliaga-Alcade, G. Christou, Science 302 (2003) 1015; (c) R. Sessoli, D. Gatteschi, A. Caneschi, M.A. Novak, Nature 365 (1993) 141; (d) Th.C. Stamatatos, K.A. Abboud, W. Wernsdorfer, G. Christou, Angew. Chem. Int. Ed. 45 (2006) 4134; (e) Th.C. Stamatatos, D. Foguet-Albiol, C.C. Stoumpos, C.P. Raptopoulou, A. Terzis, W. Wernsdorfer, S.P. Perlepes, G. Christou, J. Am. Chem. Soc. 127 (2005) 15380; (f) C.J. Milios, A. Vinslava, W. Wernsdorfer, S. Moggach, S. Parsons, S.P. Perlepes, G. Christou, E.K. Brechin, J. Am. Chem. Soc. 129 (2007) 2754; (g) P.L. Feng, C. Koo, J.J. Henderson, M. Nakano, S. Hill, E. del Barco, D.N. Hendrickson, Inorg. Chem. 47 (2008) 8610; (h) V. Mereacre, A.M. Ako, R. Clerac, W. Wernsdorfer, I.J. Hewitt, C.E. Anson, A.K. Powell, Chem. Eur. J. 14 (2008) 3577.
- [4] (a) For recent reviews, see: D. Gatteschi, R. Sessoli, Angew. Chem. Int. Ed. 42 (2003) 268; (b) G. Aromi, E.K. Brechin, Struct. Bond. 122 (2006) 1.
- [5] (a) R. Bagai, K.A. Abboud, G. Christou, Inorg. Chem. 47 (2008) 621; (b) C.J. Milios, A. Vinslava, P.A. Wood, S. Parsons, W. Wernsdorfer, G. Christou, S.P. Perlepes, E.K. Brechin, J. Am. Chem. Soc. 129 (2007) 8; (c) M. Murugesu, W. Wernsdorfer, K.A. Abboud, G. Christou, Polyhedron 24 (2005) 2894; (d) C. Lampropoulos, M. Murugesu, K.A. Abboud, G. Christou, Polyhedron 26 (2007) 2129.
- [6] (a) J.B. Vincent, H.R. Chang, K. Folting, J.C. Huffman, G. Christou, D.N. Hendrickson, J. Am. Chem. Soc. 109 (1987) 5703; (b) T. Lis, Acta Cryst. B36 (1980) 2042.
- [7] (a) A.J. Tasiopoulos, W. Wernsdorfer, K.A. Abboud, G. Christou, Angew. Chem. Int. Ed. 43 (2004) 6338; (b) A.J. Tasiopoulos, W. Wernsdorfer, K.A. Abboud, G. Christou, Inorg. Chem. 44 (2005) 6324; (c) P. King, W. Wernsdorfer, K.A. Abboud, G. Christou, Inorg. Chem. 44 (2005) 8659.
- [8] (a) N.E. Chakov, L.N. Zakharov, A.L. Rheingold, K.A. Abboud, G. Christou, Inorg. Chem. 44 (2005) 4555; (b) T.C. Stamatatos, B.S. Luisi, B. Moulton, G. Christou, Inorg. Chem. 47 (2008) 1134; (c) M. Manoli, A. Prescimone, R. Bagai, A. Mishra, M. Murugesu, S. Parsons, W. Wernsdorfer, G. Christou, E.K. Brechin, Inorg. Chem. 46 (2007) 6968; (d) T.C. Stamatatos, D. Foguet-Albiol, S.-C. Lee, C.C. Stoumpos, C.P. Raptopoulou, A. Terzis, W. Wernsdorfer, S.O. Hill, S.P. Perlepes, G. Christou, J. Am. Chem. Soc. 129 (2007) 9484.
- [9] (a) D.J. Price, S.R. Batten, B. Moubaraki, K.S. Murray, J. Chem. Soc. Chem. Commun. (2002) 762; (b) D.J. Price, S.R. Batten, B. Moubaraki, K.S. Murray, Polyhedron 22 (2003) 2161; (c) D.J. Price, S.R. Batten, B. Moubaraki, K.S. Murray, Polyhedron 26 (2007) 305; (d) A.J. Tasiopoulos, N.C. Harden, K.A. Abboud, G. Christou, Polyhedron 22 (2003) 133.
- [10] SHELXTL6; Bruker-AXS, Madison, WI, (2000).
- [11] A.J. Tasiopoulos, A. Vinslava, W. Wernsdorfer, K.A. Abboud, G. Christou, Angew. Chem. Int. Ed. 43 (2004) 2117.
- [12] (a) A.J. Tasiopoulos, W. Wernsdorfer, B. Moulton, M.J. Zaworotko, G. Christou, J. Am. Chem. Soc. 125 (2003) 15274; (b) A. Mishra, A.J. Tasiopoulos, W. Wernsdorfer, E.E. Moushi, B. Moulton, M.J. Zaworotko, K.A. Abboud, G. Christou, Inorg. Chem. 47 (2008) 4832.
- [13] W. Liu, H.H. Thorp, Inorg. Chem. 32 (1993) 4102.
- [14] A.W. Addison, T.N. Rao, J. Reedijk, J. Rijn, G.C. Verschoor, J. Chem. Soc. Dalton Trans. (1984) 1349.
- [15] (a) D.W. Low, D.M. Eichhorn, A. Draganescu, W.H. Armstrong, Inorg. Chem. 30 (1991) 877; (b) E.K. Brechin, G. Christou, M. Soler, M. Helliwell, S.J. Teat, Dalton Trans. (2003) 513; (c) H.L. Tsai, S. Wang, K. Folting, W.E. Streib, D.N. Hendrickson, G. Christou, J. Am. Chem. Soc. 117 (1995) 2503; (d) M. Murrie, S. Parsons, R.E.P. Winpenny, Dalton Trans. (1998) 1423.
- [16] (a) K.L. Taft, S.J. Lippard, J. Am. Chem. Soc. 112 (1990) 9629; (b) K.L. Taft, C.D. Delfs, G.C. Papaefthymiou, S. Foner, D. Gatteschi, S.J. Lippard, J. Am. Chem. Soc. 116 (1994) 823; (c) T.C. Stamatatos, A.G. Christou, C.M. Jones, B.J. O'Callaghan, K.A. Abboud, T.A. O'Brien, G. Christou, J. Am. Chem. Soc. 129 (2007) 9840; (d) T.C. Stamatatos, A.G. Christou, S. Mukherjee, K.M. Poole, C. Lampropoulos, K.A. Abboud, T.A. O'Brien, G. Christou, Inorg. Chem. 47 (2008) 9021.